Neurobiology of Disease

Progressive Dendritic HCN Channelopathy during Epileptogenesis in the Rat Pilocarpine Model of Epilepsy

Sangwook Jung,[1] Terrance D. Jones,[1] Joaquin N. Lugo Jr,[4] Aaron H. Sheerin,[3] John W. Miller,[1,2] Raimondo D'Ambrosio,[3] Anne E. Anderson,[4] and Nicholas P. Poolos[1,2]

[1]Department of Neurology, [2]Regional Epilepsy Center, and [3]Department of Neurological Surgery, University of Washington, Seattle, Washington 98104, and [4]Department of Pediatrics, Cain Foundation Laboratories, Baylor College of Medicine, Houston, Texas 77030

Ion channelopathy plays an important role in human epilepsy with a genetic cause and has been hypothesized to occur in epilepsy after acquired insults to the CNS as well. Acquired alterations of ion channel function occur after induction of status epilepticus (SE) in animal models of epilepsy, but it is unclear how they correlate with the onset of spontaneous seizures. We examined the properties of hyperpolarization-activated cation (HCN) channels in CA1 hippocampal pyramidal neurons in conjunction with video-EEG (VEEG) recordings to monitor the development of spontaneous seizures in the rat pilocarpine model of epilepsy. Our results showed that dendritic HCN channels were significantly downregulated at an acute time point 1 week postpilocarpine, with loss of channel expression and hyperpolarization of voltage-dependent activation. This downregulation progressively increased when epilepsy was established in the chronic period. Surprisingly, VEEG recordings during the acute period showed that a substantial fraction of animals were already experiencing recurrent seizures. Suppression of these seizures with phenobarbital reversed the change in the voltage dependence of I_h, the current produced by HCN channels, but did not affect the loss of HCN channel expression. These results suggest two mechanisms of HCN channel downregulation after SE, one dependent on and one independent of recurrent seizures. This early and progressive downregulation of dendritic HCN channel function increases neuronal excitability and may be associated with both the process of epileptogenesis and maintenance of the epileptic state.

Key words: HCN channel; epilepsy; pilocarpine; EEG; dendrites; I_h

Introduction

Every human epilepsy syndrome for which a gene mutation has been identified is associated with dysfunction in ion channel subunits (Steinlein, 2004). This fact highlights the central role of ion channelopathy in the causation of inherited epilepsy. Ion channelopathy has been hypothesized similarly to play a role in epilepsy acquired from insults to the CNS such as status epilepticus (SE). Because experimental animal models of epilepsy demonstrate an acute seizure-free interval (or "latent period") between the insult and the onset of chronic spontaneous seizures, it has been assumed that changes in ion channel expression or function occurring during the latent period may contribute to epileptogenesis, the development of the epileptic state. Numerous studies have found changes in voltage- or ligand-gated ion channels at both acute or chronic time points (Brooks-Kayal et al., 1998; Su et al., 2002; Ellerkmann et al., 2003; Bernard et al., 2004; Peng et al., 2004; Sanchez et al., 2005). In most of these studies, however, the development of spontaneous seizures was either not explicitly measured or measured using only visual observation of overt convulsions, making it difficult to establish whether the ion channel change observed was a cause or consequence of spontaneous seizures. The use of prolonged video-EEG (VEEG) monitoring, although labor intensive, allows characterization of the onset of both subtle and overt spontaneous seizures after a neural insult, and in some cases has demonstrated an epileptic phenotype in an animal model where previously seizures had not been detected (D'Ambrosio et al., 2004; Dube et al., 2006).

The hyperpolarization-activated cation (HCN) channel is a voltage-gated ion channel potentially implicated in epilepsy. I_h, the current produced by HCN channels, plays an important role in regulating neuronal excitability, particularly in hippocampal and neocortical pyramidal neurons where its high density in the apical dendrites attenuates excitatory synaptic inputs and reduces action potential (AP) firing. Loss of function of the HCN channel causes epilepsy in knock-out animals (Ludwig et al., 2003), and acquired downregulation of HCN channel function has been observed acutely after status epilepticus (Shah et al., 2004; Zhang et al., 2006). However, in neither of these recent studies was the development of spontaneous seizures evaluated; thus, it was unclear how acquired HCN channel dysfunction correlated with epileptogenesis. In the present study, we examined HCN channel properties in rat CA1 hippocampal pyramidal neurons in conjunction with VEEG recordings to monitor the development of

Received Aug. 8, 2007; revised Oct. 11, 2007; accepted Oct. 12, 2007.

This work was supported by National Institutes of Health Grants NS046604 and NS050229 (N.P.P.), NS049427 (A.E.A.), and NS053928 (R.D.) and by the Epilepsy Foundation (N.P.P.). We appreciate the technical assistance of Lindsay Warner and the helpful comments of James Bullis, Miranda Roth, and Carol Robbins on this manuscript.

Correspondence should be addressed to Nicholas P. Poolos, Department of Neurology and Regional Epilepsy Center, University of Washington, Box 359745, 325 9th Avenue, Seattle, WA 98104. E-mail: npoolos@u.washington.edu.

DOI:10.1523/JNEUROSCI.3605-07.2007

 0270-6474/07/2713012-10$15.00/0

epilepsy. Our results show that HCN channels are significantly downregulated at an acute time point 1 week postpilocarpine, with both loss of channel expression and hyperpolarization of voltage-dependent activation. This downregulation progressively increased when epilepsy was chronically established. Surprisingly, VEEG recordings during the acute period showed that a substantial fraction of animals were already experiencing recurrent seizures. Suppression of these seizures with phenobarbital (PB) reversed the change in voltage dependence of I_h, although did not affect the change in HCN channel expression. Thus, acquired HCN channelopathy after SE consists of two processes that increase excitability, one dependent on and one independent of recurrent seizures, with differing potential contributions to epileptogenesis.

Materials and Methods

Pilocarpine model. Male Sprague Dawley rats (Charles River, Wilmington, MA) were housed in a temperature-controlled vivarium on a 12 h light/dark cycle, with food and water *ad libitum*. All animal procedures were approved by the University of Washington Institutional Animal Care and Use Committee and conformed to National Institutes of Health guidelines. One hundred thirty-two rats weighing between 150 and 200 g (6–8 weeks of age) were implanted with EEG electrodes. Four epidural cortical screw electrodes (Plastics One, Roanoke, VA) were positioned bilaterally in the skull over the anterior and posterior cortex, and a reference electrode was placed ~2 mm anterior and to the right of bregma. An anchoring screw was affixed into the skull over the cerebellum. The electrode terminals were inserted into a threaded plastic pedestal (Plastics One), and the apparatus was secured onto the skull using dental acrylic. After surgery, animals were given buprenorphine (0.10 mg/kg; Bedford Laboratories, Bedford, OH) to minimize discomfort. One hundred twenty-nine of 132 (98%) animals implanted with EEG electrodes (59 acute group, 17 PB group, 56 chronic group) survived surgery. In general, animals roused from anesthesia within 2 h and were fully ambulatory and groomed by the following morning. Of the 129 animals surviving the implant procedure, two lost their electrode headset in the weeks after surgery and were killed.

After a week recovery from electrode placement, animals weighing between 150 and 250 g were given scolpolamine methylnitrate (1 mg/kg, i.p.; Sigma, St. Louis, MO) 30 min before intraperitoneal administration of pilocarpine hydrochloride (385 mg/kg; Sigma) to induce SE. The course of pilocarpine-induced SE is described previously (Leite et al., 1990; Arida et al., 1999). Briefly, within the first 15 min after pilocarpine administration, animals exhibited intense salivation, porphyrin staining of the eyes, immobility, facial automatisms, and head tremors. After 15–60 min, animals show increased head tremors with vigorous mastication, forelimb clonus, rearing, and falling with convulsive tonus of the hindlimbs. Once initiated, these behaviors occurred every 2–5 min and developed into SE by 1 h after pilocarpine injection. After 1 h in SE, seizures were terminated with diazepam (DZ; 12 mg/kg, i.p.; Hospira, Lake Forest, IL) delivered every 20 min as needed. Animals were lethargic for up to 12 h and were often ataxic and slightly dehydrated for 24 h postpilocarpine. To prevent severe dehydration, animals were given 5 ml of lactated Ringer's solution after DZ and as needed in the days after pilocarpine treatment. Sham-treated animals received scolpolamine methylnitrate and DZ injections but not pilocarpine.

Of 127 total animals treated with pilocarpine, 25 (20%) failed to achieve status within 60 min of injection and were killed. Another 25 (20%) died during SE because of intense generalized convulsions, often accompanied by bursts of wild running. Twelve (9%) animals died in the first 24 h after SE. In all, 65 of 125 (51%) animals survived the pilocarpine procedure and remained viable for recording.

VEEG recording. Animals undergoing VEEG recordings had their head sets attached to a wire cable (Plastics One) and were placed in custom acrylic cages. EEG signals were amplified with a Grass Model 8–10 D amplifier (Grass Technology, West Warwick, RI) and acquired using a PowerLab 8/30 module equipped with Chart Pro software (AD Instruments, Colorado Springs, CO). Video recording used a ZR500 digital camcorder (Canon, Lake Success, NY), which interfaced with the Chart software, allowing for synchronization of the video and EEG traces. Animals in the "acute" group were recorded for 24 h on days 3 and 6 postpilocarpine. Animals in the "chronic" groups were recorded for 24–48 h during each of weeks 3–5 postpilocarpine (see Fig. 1*A*).

Classification of seizures was conducted by visual inspection of the VEEG records according to a modified Racine scale, with event severity ranging from class 0 to class 5 (Racine, 1972). In addition to the stereotypical class 1–5 seizures described by Racine, we examined the EEG for class 0 events consisting of behavioral arrest lasting at least 10 s that was associated with a concomitant ictal alteration of the EEG signal (Hsieh and Watanabe, 2000; Dube et al., 2006). The EEG of these episodes (see Fig. 1*B*) had an abrupt onset where the amplitude increased to at least three times over baseline and consistently slowed in frequency to ~5 Hz. The end of the event occurred when the EEG once again abruptly returned to normal, at which time the animal resumed normal ambulatory behavior. The majority of these seizures lasted 10–15 s in duration. We did not score electrographic events as class 0 seizures unless they were accompanied by behavioral arrest. Similar events seen in the fluid percussion injury animal model of epilepsy were found only in epileptic animals, not controls (D'Ambrosio et al., 2004). The class 1–2 events observed generally lasted 30–40 s in length, with animals exhibiting facial twitching and/or eye blinking (class 1), as well as head nodding (class 2). The EEG frequency tended to slow, whereas the amplitude grew to at least 3.5 times baseline. After cessation of the seizure, the EEG was often somewhat attenuated in amplitude, and the animal resumed its preictal behavior. Events were not scored in which the animal's behavior could not be assessed on video (e.g., facing away from the camera).

Class 3–5 events consisted of freezing, facial twitching, back arching, and head nodding with forelimb clonus (class 3), progressing to rearing (class 4) and eventual falling with generalized convulsions (class 5). Despite these behavioral differences between seizure types, class 3–5 events had very similar EEG signatures (see Fig. 1*C*). These events usually lasted 30–60 s in duration. The EEG signal for these seizures showed amplitudes that progressed to at least five times over baseline with an accelerated frequency. As the seizure ended, the EEG abruptly attenuated in amplitude, indicative of postictal depression.

Electrophysiology and data analysis. Hippocampal slices (400 μm) were prepared from adult rats using standard procedures (Poolos and Johnston, 1999). The age ranges in postnatal weeks and number of animals in each experimental group (see Results) are as follows: control (n = 39), 6–8 weeks; acute sham (n = 10) and acute pilocarpine (n = 16), 8–10 weeks; chronic sham (n = 8) and chronic pilocarpine (n = 14), 10–14 weeks. Slices were incubated for 10 min in a holding chamber at 34°C and then kept at room temperature for 1 h before recording. Pyramidal neurons were visualized on a fixed-stage microscope (Zeiss Axioskop, Oberkochen, Germany) using differential interference contrast microscopy. All recordings were performed at 31–33°C. Recorded neurons had resting potentials between −56 and −75 mV. Whole-cell current-clamp recordings were performed using a Dagan (Minneapolis, MN) BVC-700 amplifier, sampled at 10 kHz, and filtered at 2 kHz. Cell-attached patch-clamp recordings in voltage-clamp mode were performed using an Axopatch 200A amplifier (Molecular Devices, Foster City, CA), sampled at 2 KHz, and filtered at 500 Hz. Patch pipettes made from borosilicate glass were pulled with a Sutter (Novato, CA) P-87 micropipette puller and had a resistance of 5–15 MΩ for cell-attached recordings or 5–7 MΩ for whole-cell recordings. For cell-attached recordings, pipettes were coated with Sylgard (Dow Corning, Midland, MI) to reduce pipette capacitance. Data from whole-cell recordings were used if the series resistance was <40 MΩ. The extracellular incubation and recording solutions contained the following (in mM): 125 NaCl, 25 $NaHCO_3$, 10 dextrose, 2.5 KCl, 1.25 NaH_2PO_4, 2 $CaCl_2$, and 2 $MgCl_2$, pH 7.4 (bubbled with 95% O_2 and 5% CO_2). The pipette solution for whole-cell recordings consisted of the following (in mM): 120 $KMeSO_4$, 20 KCl, 10 HEPES, 4 Na_2-ATP, 2 $MgCl_2$, 0.3 Tris-GTP, 0.2 EGTA, pH 7.3, with KOH. The pipette solution for cell-attached patch recordings contained the following (in mM): 120 KCl, 20 tetraethylammonium-Cl, 10 HEPES, 5 4-aminopyridine, 2 $CaCl_2$, 1 $MgCl_2$, 1 $BaCl_2$, pH 7.4, with KOH. All

data acquisition and analysis were performed with custom software written for the Igor Pro 4.09 analysis environment (Wavemetrics, Lake Oswego, OR). EPSPs were simulated by the use of current injections in the form of an α function: $I = I_{max}(\alpha t)(1 - e^{-\alpha t})$, where $\alpha = 1.67$. Temporal summation (TS) was calculated as the ratio of the peak amplitude of the fifth response to that of the first. Estimation of patch area obtained from pipette resistance was used to calculate I_h density (pA/μm^2) (Sakmann and Neher, 1995). We did not correct membrane potentials for calculated liquid junction potentials of 2 mV (cell-attached recordings) or 9 mV (whole-cell recordings). All of the values are presented as the means ± SE. Statistical significance was determined by Student's *t* test (unpaired, two-tailed) or a one-way ANOVA with subsequent Tukey's *post hoc* analysis.

Western blotting. At the acute and chronic periods after SE, experimental and sham-injected animals were killed, and the hippocampus was removed and frozen. The hippocampi were then thawed in homogenization buffer (20 mM Tris-HCl at pH 7.5, 1 mM EGTA, 1 mM EDTA, 25 μg/ml aprotonin, 25 μg/ml leupeptin, 1 mM $Na_4P_2O_7$, 500 μM PMSF, 4 mM para-nitrophenylphosphate, 1 mM sodium orthovanadate), and the CA1 region of the hippocampus was microdissected (Lubin et al., 2007). CA1 tissue samples were homogenized in 500 μl of homogenatization buffer, normalized using a Bradford assay, and membranes prepared as described previously (Varga et al., 2000). The membrane samples from the experimental and control groups were loaded and run on a 10% acrylamide gel. Gels were then blotted electrophoretically to Immobilon-P filter paper (Millipore, Billerica, MA) with a transfer tank (transfer buffer: 192 mM glycine, 25 mM Tris at pH 8.3) maintained at 4°C. The gels were transferred overnight (12–18 h) at a constant current of 300 mA. They were then blocked for 1 h at room temperature in Blotto (10 mM Tris-HCl at pH 7.5, 150 mM NaCl, 0.05% Tween 20, 5% powdered milk, and 0.01% thimerosal). The Immobilon paper was incubated with either HCN1 or HCN2 antibodies (Chemicon, Temecula, CA) at a dilution of 1:500, followed by incubation in anti-rabbit secondary antibody (Cell Signaling Technology, Beverly, MA) at a dilution of 1:40,000. The Immobilon paper was then developed by enhanced chemiluminescence (ECL; GE Healthcare, Piscataway, NJ) or through SuperSignal (Pierce, Rockford IL), stripped and reprobed using anti-actin antibodies (1:10,000; Sigma, St Louis, MO), followed by incubation in anti-rabbit secondary antibody (Cell Signaling Technology) at a dilution of 1:40,000. Bands corresponding to the full-length HCN1 (117 kDa) and HCN2 (97 kDa) subunits were densitized using NIH Image software and normalized to actin immunoreactivity.

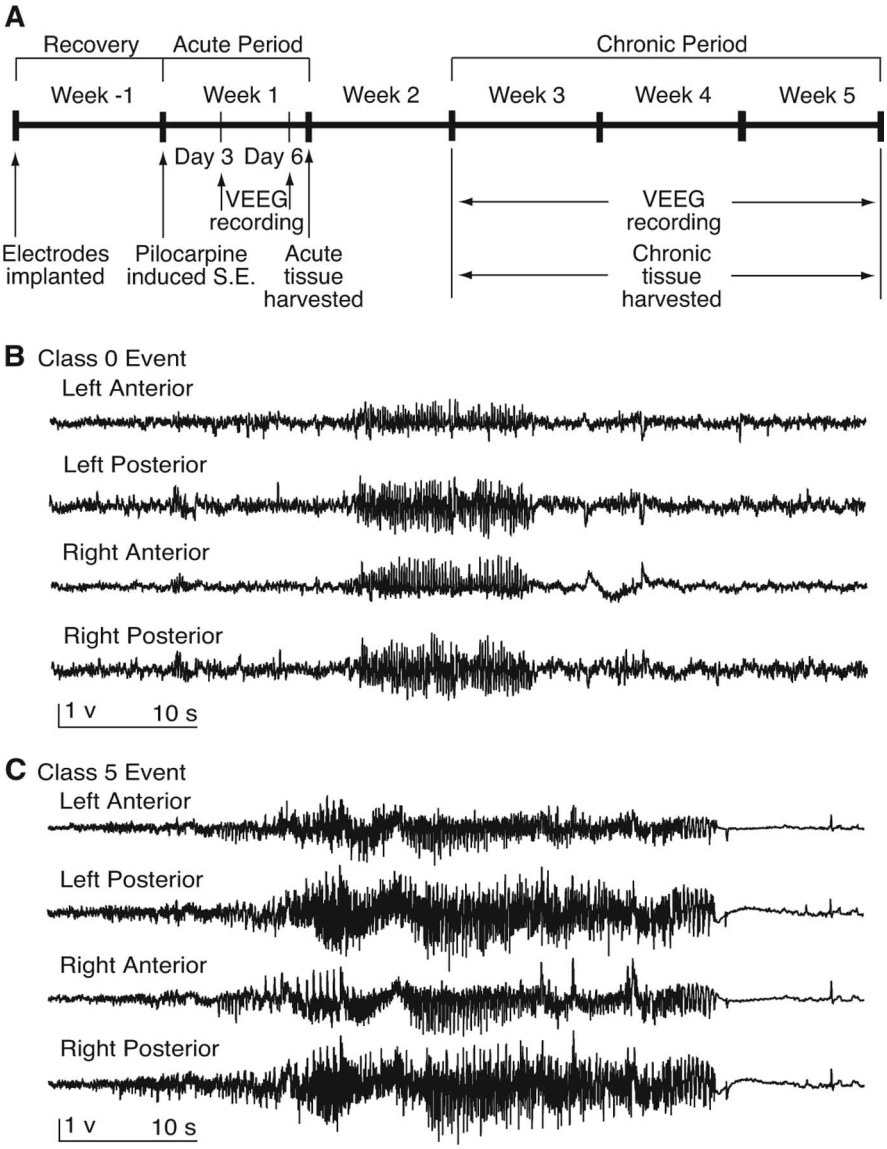

Figure 1. Chronology of procedures and characteristic EEG events. ***A***, Timeline of procedures. ***B***, EEG trace of an electrographic seizure corresponding to a Racine class 0 event associated with behavioral arrest lasting ~13 s. Note the abrupt onset and end of the seizure, as well as generally uniform spiking amplitude three times that of baseline. Predominant spike frequency was 5 Hz. Trace labels indicate electrode position. ***C***, EEG trace of an electrographic seizure corresponding to a class 5 event with a generalized convulsion ~40 s in duration. The seizure discharge progressively grows in amplitude to five times over baseline, with frequency that increases up to 10 Hz and then slows as the seizure progresses. EEG amplitude is greatly attenuated after the event, indicative of postictal depression.

Results

Spontaneous seizures occur during the first week postpilocarpine

To determine whether acquired changes in HCN channel function occur during the development of the epileptic state after SE, we investigated the electrophysiological properties and protein expression of HCN channels and used VEEG recordings to observe the onset of seizure activity in pilocarpine-treated animals. First, we performed VEEG monitoring of animals in the "acute" timeframe during the first week after pilocarpine treatment (Fig. 1*A*) to determine the occurrence of seizures during a period usually considered within the seizure-free "latent period" of ~15 d (Leite et al., 1990). Concurrently with the VEEG monitoring, hippocampal tissue was harvested at 7 d postpilocarpine to assess the properties in I_h. Animals were also recorded in the "chronic" period 3- 5 weeks after pilocarpine treatment to identify chronically epileptic animals for tissue harvest to measure I_h.

VEEG monitoring was conducted for ~2600 h in total. For purposes of analysis, we grouped seizure types into those with subtle behavioral manifestations (Racine class 0–2) and those with overt motor activity (Racine class 3–5; see Materials and Methods for details). Pilocarpine-treated rats exhibited both class

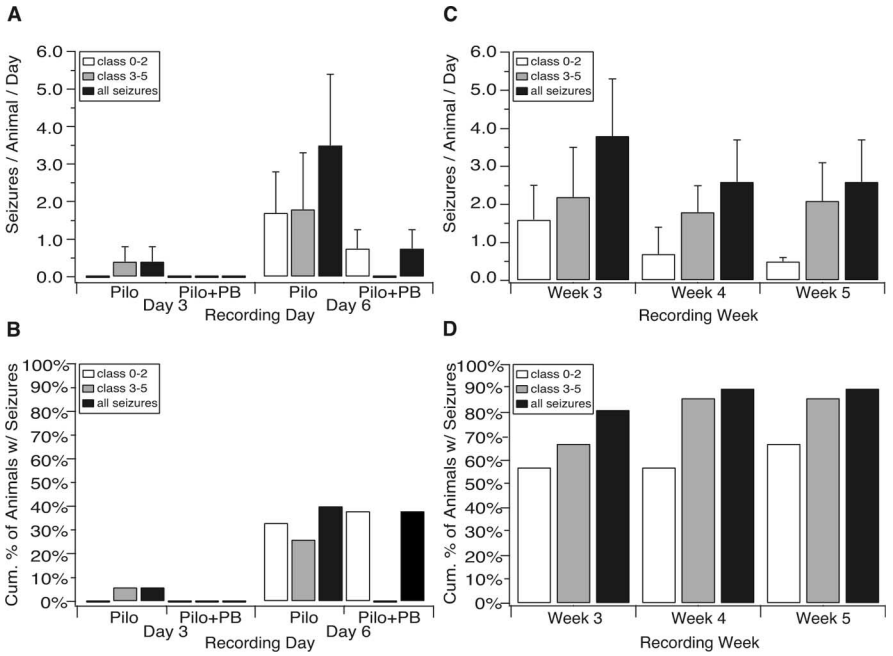

Figure 2. Spontaneous seizures begin during the acute period 1 week postpilocarpine. ***A***, Histogram showing the number of seizures per all animals monitored during the acute period. Both class 0–2 and class 3–5 seizures were evident in the first week postpilocarpine. Seizure activity was reduced in animals also receiving PB during the first week after pilocarpine compared with animals that received pilocarpine alone. ***B***, Cumulative percentage of animals that experienced seizures during the first week postpilocarpine. Forty percent of pilocarpine-only-treated animals experienced seizures, whereas 38% of pilocarpine-treated animals that received PB in the first week postpilocarpine had seizures, although all of these seizures were of class 0–2. ***C***, Number of seizures per animal monitored during the chronic period. At week three, class 0–2 events had declined in frequency, and by 5 weeks postpilocarpine, ictal activity had mostly shifted to class 3–5 events. ***D***, Cumulative percentage of animals developing seizures during the chronic period. By 5 weeks postpilocarpine, 91% of animals had experienced a spontaneous seizure.

0–2 and class 3–5 seizures during the acute period. As shown in Figure 1*B*, a typical class 0 event consisted of the abrupt onset of an electrographic discharge, associated with sudden immobility in a previously behaving animal, followed by resumption of normal behavior at the end of the discharge. A typical class 5 event (Fig. 1*C*) was characterized by a gradually evolving, more prolonged discharge, associated with clonic movements, followed by rearing and falling. After the seizure, the EEG signal was attenuated, and the animal displayed postictal lethargy.

Fifteen animals were recorded for 24 h each on days 3 and 6 postpilocarpine (Fig. 2*A*,*B*). One animal (7% of animals) exhibited six class 3–5 events on day 3 (0.4 ± 0.4 seizures per all animals recorded; $n = 15$). On day 6, five animals had experienced class 0–2 seizures (33% of animals), ranging in frequency from 1 to 17 per animal (1.7 ± 1.1 seizures; $n = 15$). Four animals (27%) had class 3–5 events, with a frequency range of 1–22 per animal (1.8 ± 1.5; $n = 15$). Some animals experienced both class 0–2 and class 3–5 seizures on day 6. Class 0 events composed 11% of all seizures on day six. In total, six animals (40% of total) had either a class 0–2 or class 3–5 event within the first week postpilocarpine (3.5 ± 1.9; $n = 15$). This proportion of animals with recurrent seizures within the first week postpilocarpine is likely an underestimate of the true frequency, because we conducted VEEG monitoring on only 2 of 7 days. In comparison, a recent study that used continuous VEEG monitoring in the first 15 d after pilocarpine treatment, but excluded class 0 events from analysis, found a median latency period of 6 d (Goffin et al., 2007). Also, focal hippocampal seizures may occur undetected by the epidural surface electrodes used in this study (Leite et al., 1990; Dube et al., 2006), thus potentially leading to further underestimates of the true seizure frequency. For these reasons, at least 50%, and possibly a greater fraction of our animals, were likely epileptic by day 7.

Because of the unexpectedly high proportion of animals observed to have seizures in the acute period, we administered the antiepileptic drug PB (55 mg/kg, s.c., twice a day starting 24 h postinduction) to a second group of animals during the first week postpilocarpine, as a later control for the effects of seizures on electrophysiological and biochemical measurements. Serum trough levels of PB were found to be within therapeutic range (15–40 μg/ml) (MacDonald and McLean, 1986) when measured at 3 d (39.4 ± 5.8 μg/ml; $n = 3$) and 6 d (31.4 ± 6.4 μg/ml; $n = 5$) postpilocarpine. Administration of PB markedly reduced ictal activity during the acute period (Fig. 2*A*,*B*). Of the nine animals receiving PB that were recorded on day 3, no animals had either class 0–2 or class 3–5 events. On day 6, no class 3–5 seizures were observed, although three animals in eight (38% of animals) experienced a class 0–2 seizure (0.75 ± 0.49 seizures; $n = 8$). In summary, VEEG recording during the acute period revealed that a significant proportion of animals had seizures in the first week postpilocarpine, and administration of PB markedly reduced the frequency and severity of ictal events in pilocarpine-treated animals.

During the chronic period beginning 3 weeks postpilocarpine, animals exhibited both class 0–2 and class 3–5 events, with the frequency of class 0–2 events declining throughout the chronic period, whereas class 3–5 events remained approximately constant in frequency (Fig. 2*C*). In week 3, six animals showed class 0–2 events (1.6 ± 0.9 seizures per animal per day; $n = 21$), whereas eight animals had class 3–5 events (2.2 ± 1.3; $n = 21$). At week 4, two animals experienced class 0–2 seizures (0.7 ± 0.7; $n = 15$), whereas seven animals had class 3–5 seizures (1.8 ± 0.7; $n = 15$). At the end of chronic period 5 weeks postpilocarpine, class 3–5 events still predominated (2.1 ± 1.0; $n = 14$), whereas class 0–2 seizures diminished further (0.5 ± 0.1; $n = 14$).

The incidence of seizures was tallied for the animals recorded throughout the 3 weeks of the chronic period, including data on seizure incidence in week 2 postpilocarpine (data not shown), to estimate the cumulative likelihood of an animal becoming epileptic after the acute period (Fig. 2*D*). Eighty-one percent of pilocarpine-treated animals exhibited spontaneous seizures by week 3. By 5 weeks postpilocarpine, 91% of animals had developed epilepsy. It should be noted that the cumulative incidence of epilepsy in these animals is likely an underestimate of the true incidence, because these figures do not count seizures in the first week postpilocarpine (these animals were killed for acute period experiments), and chronic period animals were recorded on only 1 or 2 d of each subsequent week. Together, these results indicate that the average latent period postpilocarpine is likely less than 7 d, and the frequency of all seizure types combined achieved a plateau by day 6 postpilocarpine that remained approximately constant in weeks 3–5, although average seizure severity wors-

ened. Virtually all animals were epileptic by the end of the chronic period. VEEG monitoring promoted a more comprehensive quantification of the course of epileptogenesis, especially during the acute period, than is achieved with visual monitoring only by allowing detection of short, subtle ictal events such as the class 0–2 seizures seen here.

I_h is significantly reduced in pyramidal neuron dendrites in the acute period postpilocarpine

Concurrently with our VEEG monitoring, we investigated whether I_h is altered in hippocampal pyramidal neurons during the acute period 1 week after pilocarpine-induced SE. Because of our initial expectation that few animals would have seizures during the acute period, and our intent to avoid the potentially confounding effects of seizures on HCN channel properties, we used pilocarpine-treated animals at 7 d for cell-attached patch-clamp recordings only if they lacked spontaneous seizures on days 3 and 6 of VEEG monitoring. However, given the surprising frequency of seizures seen during the acute period in the pilocarpine-treated animal population (Fig. 2), it is likely that many of the animals used for electrophysiology did experience seizures on other days during the acute period, as discussed above. Because I_h is predominantly localized to the apical dendrites of CA1 hippocampal pyramidal neurons (Magee, 1998), we performed dendritic cell-attached patch-clamp recordings in hippocampal CA1 pyramidal neurons from brain slices of pilocarpine-treated, age-matched sham-injected, and naive animals.

The voltage-dependent activation of I_h was similar in both naive and age-matched sham-injected animals (Fig. 3*A*). The I_h half-activation voltage ($V_{1/2}$) in pyramidal neuron dendrites from naive animals was not significantly different from that in sham-injected animals (control, -91 ± 1.8 mV, $n = 19$; acute sham, -92 ± 2.5 mV, $n = 6$; $p > 0.05$) (Fig. 3*B*), suggesting that intrinsic I_h properties of sham-injected animals were similar to those of naive animals (Fig. 3*C–E*). However, the voltage-dependent activation of I_h in pyramidal neuron dendrites from pilocarpine-treated animals showed a hyperpolarized shift compared with sham-injected animals (Fig. 3*B*). The $V_{1/2}$ from pilocarpine-treated animals was also significantly hyperpolarized compared with sham-injected animals ($V_{1/2}$: in acute pilocarpine, -98 ± 1.3 mV, $n = 10$; in acute sham, -92 ± 2.5 mV, $n = 6$; $p < 0.05$) (Fig. 3*B*), implying a decrease in activated HCN channels at resting membrane potential (RMP) (-60 to -70 mV). The dendritic recording distances from the soma in naive, sham-injected, and pilocarpine-treated animals were similar: 209 ± 5.6 μm, $n = 19$; 183 ± 8.4 μm, $n = 6$; and 188 ± 5.9 μm, $n = 10$, respectively.

I_h current density was measured at hyperpolarized potentials where voltage-dependent activation was maximal. The I_h current density measured in pyramidal neuron dendrites from pilocarpine-treated animals was significantly reduced compared with sham-injected animals (control, 30 ± 3.0 pA/μm^2, $n = 19$; acute sham, 28 ± 4.5 pA/μm^2, $n = 6$; acute pilocarpine, 12 ± 2.4 pA/μm^2, $n = 10$; $p < 0.01$) (Fig. 3*C*). After cell-attached patch recording, the patch was ruptured to determine the RMP. The RMP in pyramidal neuron dendrites from pilocarpine-treated animals was -67 ± 1.5 mV ($n = 5$), which was significantly hyperpolarized compared with sham-injected animals (control, -60 ± 1.1 mV, $n = 13$; acute sham, -62 ± 1.4 mV, $n = 5$; $p < 0.05$) (Fig. 3*D*), consistent with downregulation of HCN channels and their contribution to the RMP in neurons (Lupica et al., 2001; Day et al., 2005).

I_h in CA1 hippocampal pyramidal neurons shows fast and slow activation time constants, reflecting the expression of both HCN1 and HCN2 subtypes, with the HCN1 subtype showing faster kinetics than the HCN2 subtype (Santoro and Tibbs, 1999). The currents evoked near $V_{1/2}$ were fitted to double exponential functions to determine activation time constants, and current decay was fitted with a single exponential function to measure deactivation time constants. In the acute period postpilocarpine, fast and slow activation time constant components were significantly increased compared with those from sham-injected animals (Fig. 3*E*; Table 1). There was no significant difference in I_h deactivation time constants between sham-injected and pilocarpine-treated animals (Fig. 3*E*; Table 1). These results show that during the acute period, 1 week postpilocarpine, there is a downregulation of HCN channel function in the CA1 pyramidal neuron dendrites with a hyperpolarized shift in voltage-dependent activation of I_h, slowing of activation, and a significant loss of I_h density.

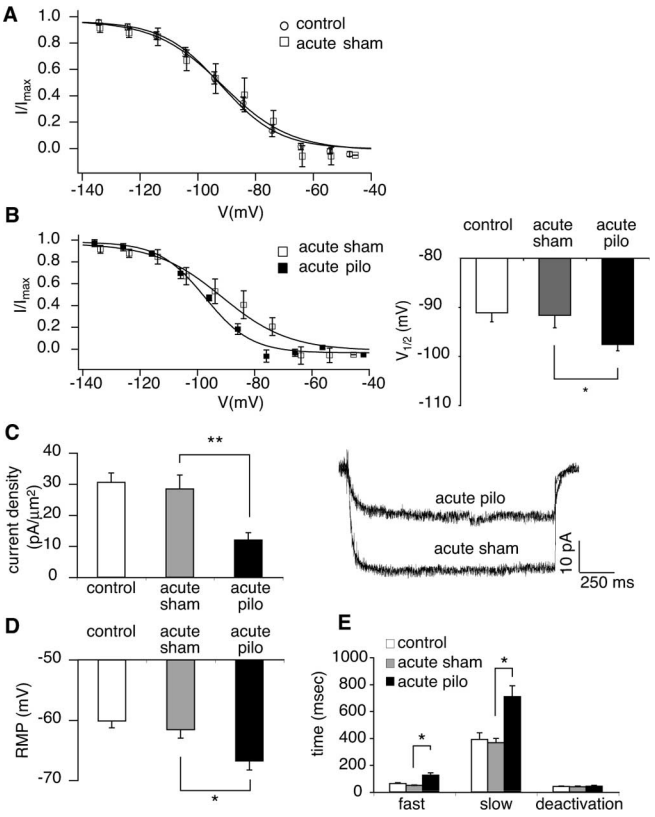

Figure 3. Downregulation of I_h at 1 week postpilocarpine (acute period). ***A***, Voltage-dependent activation of I_h in dendrites of CA1 hippocampal pyramidal neurons from naive animals (control; circles) was similar to that from age-matched sham-injected animals (acute sham; squares). ***B***, I_h voltage-dependent activation from pilocarpine-treated animals in the acute period (acute pilo; solid squares) was hyperpolarized compared with sham-injected animals (acute sham; open squares; $^*p < 0.05$). ***C***, I_h density obtained from postpilocarpine animals in the acute period was significantly reduced compared with sham-injected animals ($^{**}p < 0.01$). Representative current traces shown are from voltage commands of -152 and -157 mV in pyramidal neuron dendrites from sham-injected and pilocarpine-treated animals, respectively. The dendritic recording distances were 180 and 200 μm, respectively. ***D***, The RMP in pyramidal neuron dendrites from pilocarpine-treated animals showed a hyperpolarized shift compared with the RMP of sham-injected animals ($^*p < 0.05$), consistent with I_h downregulation. ***E***, I_h activation time constants (fast and slow) measured near $V_{1/2}$ in pyramidal neuron dendrites from pilocarpine-treated animals were increased compared with those of sham-injected animals ($^*p < 0.05$). I_h deactivation time constants were similar in sham-injected and pilocarpine-treated animals.

Table 1. I_h activation (fast and slow) and deactivation time constants measured at $V_{1/2}$ in pyramidal neuron dendrites from naive animals (control), pilocarpine-treated animals during acute and chronic periods (acute pilo and chronic pilo), and age-matched sham-injected animals (acute or chronic sham)

	Fast (ms)	Slow (ms)	Deactivation (ms)
Control	63.6 + 5.27 ($n = 18$)	390 + 48.9 ($n = 18$)	40.8 + 3.22 ($n = 18$)
Acute sham	49.9 + 2.51 ($n = 6$)	366 + 32.7 ($n = 6$)	38.7 + 5.79 ($n = 6$)
Acute pilo	125 + 18.4 ($n = 10$)	708 + 81.8 ($n = 10$)	42.9 + 6.22 ($n = 10$)
Acute sham versus pilo	$p < 0.05$	$p < 0.05$	n.s.
Chronic sham	61.4 + 8.01 ($n = 8$)	396 + 60.4 ($n = 8$)	37.6 + 3.88 ($n = 8$)
Chronic pilo	94.6 + 21.3 ($n = 6$)	706 + 50.9 ($n = 6$)	53.8 + 6.75 ($n = 6$)
Chronic sham versus pilo	n.s.	$p < 0.05$	n.s.

I_h is further reduced in pyramidal neuron dendrites in the chronic period postpilocarpine

We then examined whether the changes in the biophysical properties of HCN channels observed during the acute period postpilocarpine in dendrites of CA1 hippocampal pyramidal neurons continued in the chronic period 3–5 weeks postpilocarpine when recurrent seizures were established in virtually all animals. The tissue harvest dates in sham-injected and pilocarpine-treated animals during the chronic period were 29 ± 7.0 d ($n = 8$) and 24 ± 7.0 d ($n = 6$) postinduction, respectively. For pilocarpine-treated animals, we performed electrophysiological recordings in CA1 hippocampal pyramidal neurons only from animals showing spontaneous seizures, as confirmed by VEEG analysis. The voltage-dependent activation of I_h in CA1 pyramidal neuron dendrites from chronic sham-injected animals was similar to that of naive animals (Fig. 4*A*), with $V_{1/2}$ in sham-injected animals not significantly different from that in naive animals (chronic sham, −93 ± 3.0 mV, $n = 8$; control, −91 ± 1.8 mV, $n = 19$; $p > 0.05$), suggesting that intrinsic I_h properties in pyramidal neuron dendrites of chronic sham-injected animals were similar to that of naive animals. The voltage-dependent activation of I_h in CA1 pyramidal neuron dendrites from chronically epileptic animals showed a hyperpolarized shift, compared with sham-injected animals, which was similar to but more pronounced than that seen during the acute period postpilocarpine (Fig. 4*B*). Likewise, the $V_{1/2}$ from pilocarpine-treated animals was increasingly hyperpolarized compared with that of sham-injected animals (chronic pilocarpine, −105 ± 3.5 mV, $n = 6$; chronic sham, −93 ± 3.0 mV, $n = 8$; $p < 0.05$) (Fig. 4*B*). The dendritic recording distances in sham-injected and pilocarpine-treated animals were similar, 178 ± 6.8 μm ($n = 8$) and 172 ± 4.8 μm ($n = 6$), respectively.

As in animals evaluated during the acute period postpilocarpine, the maximal I_h current density measured in CA1 pyramidal neuron dendrites from epileptic animals during the chronic period postpilocarpine was also significantly reduced compared with sham-injected animals (control, 30 ± 3.0 pA/μm^2, $n = 19$; chronic sham, 26 ± 3.2 pA/μm^2, $n = 8$; chronic pilocarpine, 9.7 ± 2.1 pA/μm^2, $n = 6$; $p < 0.01$) (Fig. 4*C*). The RMP determined in pyramidal neuron dendrites from pilocarpine-treated animals was −73 ± 0.6 mV ($n = 5$), which was significantly hyperpolarized compared with the RMP of sham-injected animals (control, −60 ± 1.1 mV, $n = 13$; chronic sham, −60 ± 1.0 mV, $n = 8$; $p < 0.05$) (Fig. 4*D*), again consistent with I_h downregulation. This RMP hyperpolarization was also increased compared with the acute period.

The slow component of I_h activation time constants obtained during the chronic period was significantly increased compared with that of sham-injected animals (Fig. 4*E*; Table 1). Fast activation time constants were not significantly different in sham-injected and pilocarpine-treated animals. There was also no difference between I_h deactivation time constants (Fig. 4*E*; Table 1).

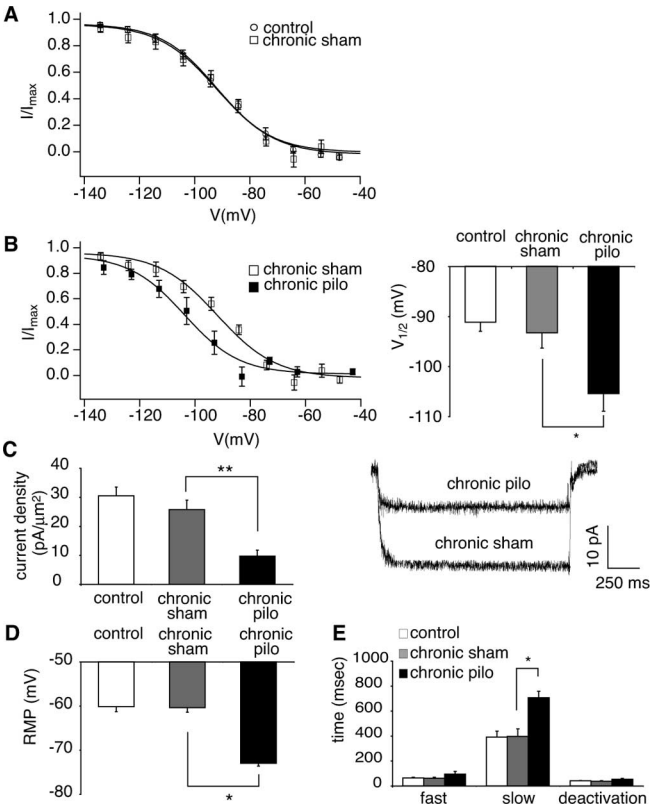

Figure 4. Downregulation of I_h at 3–5 weeks postpilocarpine (chronic period). ***A***, Voltage-dependent activation of I_h in dendrites of CA1 hippocampal pyramidal neurons from naive animals (control; circles) was similar to that from age-matched sham-injected animals (chronic sham; squares). ***B***, I_h voltage-dependent activation from pilocarpine-treated animals in the chronic period (chronic pilo; solid squares) was hyperpolarized compared with sham-injected animals (chronic sham; open squares; $*p < 0.05$). ***C***, I_h density obtained from pilocarpine-treated animals was significantly reduced compared with sham-injected animals ($**p < 0.01$). Current traces shown are from voltage commands of −150 and −153 mV in pyramidal neuron dendrites from sham-injected and pilocarpine-treated animals, respectively. The dendritic recording distance in both sham-injected and pilocarpine-treated animals was 160 μm. ***D***, The RMP in pyramidal neuron dendrites from pilocarpine-treated animals was significantly hyperpolarized compared with that of sham-injected animals ($*p < 0.05$), consistent with I_h downregulation. ***E***, Slow but not fast I_h activation time constants of pilocarpine-treated animals were increased compared with those of sham-injected animals ($*p < 0.05$). I_h deactivation time constants were similar in both sham-injected and pilocarpine-treated animals.

These results show that the downregulation of I_h first observed during the acute period postpilocarpine, evidenced by hyperpolarized $V_{1/2}$ and decreased current density, persists to the chronic period when animals uniformly experience recurrent seizures. The voltage-dependent activation and RMP are increasingly hyperpolarized at chronic compared with acute time points.

We also measured I_h at the soma of CA1 hippocampal pyramidal neurons during epileptogenesis. We found no significant

difference in I_h density at the soma of CA1 hippocampal pyramidal neurons between sham-injected and pilocarpine-treated animals during the acute (acute sham, 5.0 ± 1.5 pA/μm^2, $n = 7$; acute pilocarpine, 4.7 ± 0.4 pA/μm^2, $n = 9$) or chronic (chronic sham, 6.3 ± 1.3 pA/μm^2, $n = 5$; chronic pilocarpine, 5.2 ± 0.6 pA/μm^2, $n = 5$) periods postpilocarpine. Voltage-dependent activation of I_h at the soma was also similar in sham-injected and pilocarpine-treated animals ($V_{1/2}$ in acute sham, −91 ± 1.9 mV, $n = 7$; acute pilocarpine, −92 ± 2.9 mV, $n = 9$; chronic sham, −94 ± 4.9 mV, $n = 5$; chronic pilocarpine, −91 ± 7.1 mV, $n = 5$). Thus, unlike the case for dendritic I_h, somatic I_h properties were unchanged during epileptogenesis.

The expression of HCN channel subunits is reduced during the acute and chronic periods

To determine whether the reduction of I_h density in the acute and chronic periods represented a decreased number of HCN channels, we examined the expression of HCN1 and HCN2 subunits with Western blotting. For these biochemical studies, animals underwent the same pilocarpine protocol and were examined at the same time points as those that were used for electrophysiological experiments, but most of these animals did not undergo VEEG monitoring. CA1 hippocampal HCN1 and HCN2 protein expression measured during the acute period at 7 d postpilocarpine were significantly reduced compared with sham-injected animals (for HCN1: acute sham, 100 ± 6.68%, $n = 10$; acute pilocarpine, 57 ± 9.6%, $n = 6$, $p < 0.01$; for HCN2: acute sham, 100 ± 5.33%, $n = 10$; acute pilocarpine, 44 ± 7.5%, $n = 9$; $p < 0.01$) (Fig. 5*A*). This reduction of HCN channel expression was similar to that of I_h density during the acute period (44–57% of control in HCN channel expression; 43% of control in I_h density), suggesting that the decreased I_h density observed during the acute period reflected a loss of HCN channel subunits. An analysis of HCN1 and HCN2 protein expression from epileptic animals during the chronic period 3–5 weeks postpilocarpine also showed a significant reduction in HCN1 protein compared with sham-injected animals (chronic sham, 100 ± 14.9%, $n = 7$; chronic pilocarpine, 53 ± 7.1%, $n = 5$; $p < 0.05$) (Fig. 5*B*). In contrast, no change in HCN2 protein expression during the chronic period was found between sham-injected and pilocarpine-treated animals (chronic sham, 100 ± 8.85%, $n = 7$; chronic pilocarpine, 99 ± 19%, $n = 5$) (Fig. 5*B*), suggesting that the decreased HCN2 expression seen during the acute period had reverted to normal.

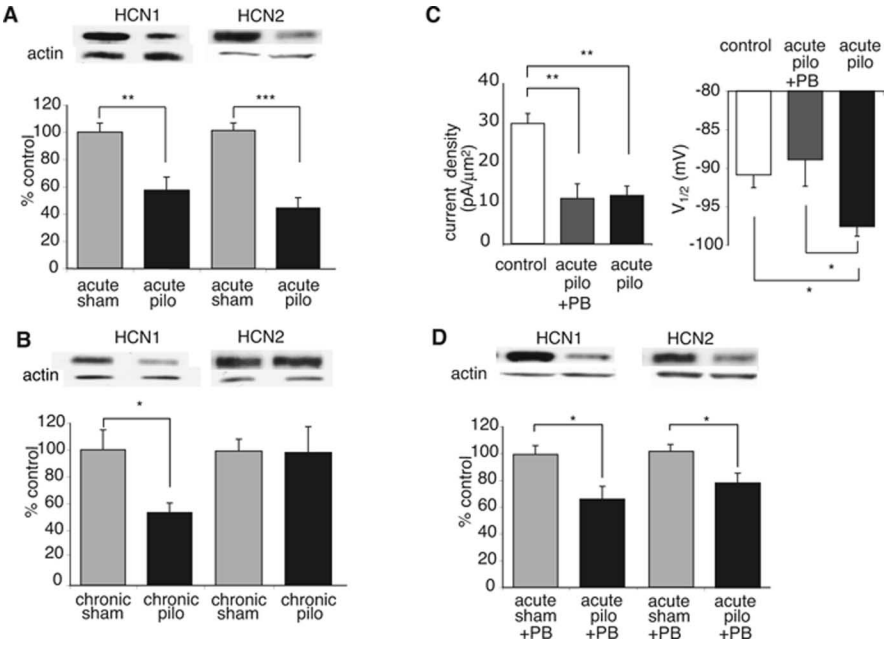

Figure 5. Decreased HCN protein expression at acute and chronic periods after pilocarpine treatment. ***A***, HCN1 and HCN2 protein expression in CA1 hippocampal tissue was decreased in pilocarpine-treated animals compared with sham-injected animals at the acute period (**$p < 0.01$ and ***$p < 0.001$). Representative blots of HCN1, HCN2, and actin protein expression are shown in each condition. ***B***, HCN1 but not HCN2 protein expression remained reduced during the chronic period compared with age-matched sham-injected tissue (*$p < 0.05$). ***C***, I_h density obtained from animals treated with PB during the acute period postpilocarpine (acute pilo+PB) was significantly reduced compared with control (**$p < 0.01$), similar to rats treated with pilocarpine alone (acute pilo; **$p < 0.01$, one-way ANOVA with Tukey's *post hoc* test). Unlike I_h density, $V_{1/2}$ in pilocarpine-treated animals with PB was unchanged from control and different from rats treated with pilocarpine alone (*$p < 0.05$, one-way ANOVA with Tukey's *post hoc* test). ***D***, HCN1 and HCN2 protein expression in animals receiving PB during the acute period postpilocarpine was decreased compared with sham-injected animals treated with PB only (*$p < 0.05$). Loss of HCN1/2 expression was similar in pilocarpine-treated animals with PB as in those treated with pilocarpine alone.

Seizure dependence of HCN channel gating changes

Because spontaneous seizures were observed during the acute period in a significant proportion of animals, we then asked whether the downregulation of HCN channels was a result of ongoing seizures. Pilocarpine-treated rats treated with the antiepileptic drug PB during the acute period showed a marked suppression of spontaneous seizures (Fig. 2*A*,*B*). We then killed these animals for electrophysiological recording and Western blot analysis. I_h properties were found to be similar in naive and sham-injected animals with PB; therefore, these data were pooled for control data in this experiment (I_h density in naive animals, 30 ± 3.0 pA/μm^2, $n = 19$; in sham-injected animals with PB, 27 ± 2.5 pA/μm^2, $n = 4$, $p > 0.05$; $V_{1/2}$ in naive animals, −91 ± 1.8 mV, $n = 19$; in sham-injected animals with PB, −89 ± 4.6 mV, $n = 4$, $p > 0.05$). Pilocarpine-treated animals given PB showed decreased dendritic I_h density compared with control, similar to animals treated with pilocarpine alone (acute pilocarpine plus PB, 11 ± 3.6 pA/μm^2, $n = 6$; control, 30 ± 2.5 pA/μm^2, $n = 23$; acute pilocarpine, 12 ± 2.4 pA/μm^2, $n = 10$; $p < 0.01$ compared by one-way ANOVA) (Fig. 5*C*), demonstrating that the decreased I_h density observed during the acute period after pilocarpine treatment was not influenced by ongoing seizures. Interestingly, the voltage-dependent activation of I_h in pilocarpine-treated rats given PB was similar to that of control, unlike animals treated with pilocarpine alone ($V_{1/2}$ in acute pilocarpine plus PB, −89 ± 3.5 mV, $n = 6$; in control, −91 ± 1.7 mV, $n = 23$; in acute pilocarpine, −98 ± 1.3 mV, $n = 10$; $p < 0.05$ compared by one-way ANOVA) (Fig. 5*C*). The dendritic recording distances in control, pilocarpine-treated animals given PB, and pilocarpine-treated animals were similar: 210 ± 4.8 μm, $n = 23$; 178 ± 23 μm, $n = 6$; and 188 ± 5.9 μm, $n = 10$, respectively.

HCN1 and HCN2 protein expression from pilocarpine-treated animals given PB were also decreased compared with sham-injected animals given PB, consistent with the decreased I_h density seen in PB-treated animals postpilocarpine (HCN1 pro-

tein expression, acute sham plus PB, 99 ± 5.9%, $n = 5$; acute pilocarpine plus PB, 66 ± 7.6%, $n = 11$, $p < 0.05$; HCN2 protein expression, acute sham plus PB, 104 ± 6.50%, $n = 8$; acute pilocarpine plus PB, 80 ± 8.4%, $n = 9$, $p < 0.05$) (Fig. 5*D*). Together, these results suggest that HCN channels are significantly downregulated during the acute period after SE in the rat pilocarpine model, with both loss of channel expression and alteration of I_h voltage-dependent activation. The downregulation of I_h persisted to the chronic period postpilocarpine, with the decrease of I_h density during the acute and chronic periods directly linked to loss of HCN subunits in CA1 hippocampal pyramidal neurons. Suppression of seizures with PB showed that changes in the voltage-dependent activation of I_h during the acute period after pilocarpine-induced SE were dependent on spontaneous seizure activity, whereas the loss of I_h density and expression of HCN channels were independent of spontaneous seizures.

Dendritic hyperexcitability is associated with downregulation of I_h in pilocarpine-treated animals

We then determined how downregulation of HCN channels affected the excitability of CA1 hippocampal pyramidal neurons from chronically epileptic animals. Two parameters sensitive to the amount of I_h active at rest, input resistance (IR) and TS of EPSP-like voltage transients, were examined through current-clamp recordings in pyramidal neuron dendrites from epileptic animals at 18–21 d (chronic period) postpilocarpine. Previous data in this study showed that the biophysical properties of HCN channels were similar in both naive and chronic sham-injected animals (Fig. 4); thus, we used naive animals for control data in these experiments. For current-clamp recordings, $KMeSO_4$ solution was used for the pipette internal solution because K-gluconate blocks I_h and some K^+ currents (Velumian et al., 1997). The dendritic recording distances were similar in control and epileptic animals: 173 ± 5.1 μm ($n = 20$) and 174 ± 9.9 μm ($n = 8$), respectively.

Hyperpolarizing current pulses in pyramidal neuron dendrites from control and pilocarpine-treated animals resulted in a depolarizing "sag" in the voltage response that indicated the presence of I_h (Fig. 6*A*) (Magee, 1998). The steady-state IR was determined in response to hyperpolarizing current pulses (100–300 pA current commands) applied from a holding potential of −65 mV. The IR in CA1 pyramidal neuron dendrites from epileptic animals during the chronic period postpilocarpine was significantly higher than that in control animals (control, 51 ± 3.4 MΩ, $n = 20$; chronic pilocarpine, 71 ± 15.8 MΩ, $n = 8$, $p < 0.05$), consistent with the observed decrease in I_h. We then tested whether temporal summation of EPSP-like voltage transients was affected in the chronic period postpilocarpine. I_h influences temporal summation of EPSPs and produces maximal effect on TS at a frequency of 20 Hz in CA1 pyramidal neuron dendrites (Magee, 1998; Poolos et al., 2002). Trains of five α function currents at 20 Hz were injected into the dendrites of CA1 hippocampal pyramidal neurons to simulate EPSPs. TS was measured as the ratio of the fifth response amplitude to that of the first. Somewhat to our surprise, there was no significant difference in TS between control and epileptic animals during the chronic period (control, 120 ± 4.5%, $n = 20$; chronic pilocarpine, 120 ± 8.7%; $n = 8$; $p > 0.05$).

Finally, we investigated the relationship between dendritic current injection and AP firing in control and epileptic animals to look for evidence of enhanced dendritic excitability in pyramidal neuron dendrites after pilocarpine-induced SE. There was a significantly higher frequency of AP firing in CA1 hippocampal pyramidal neurons from epileptic animals compared with control animals (Fig. 6*C*). These results suggest that the increase in IR associated with downregulation of HCN channels after pilocarpine treatment is associated with enhanced dendritic excitability in pyramidal neurons.

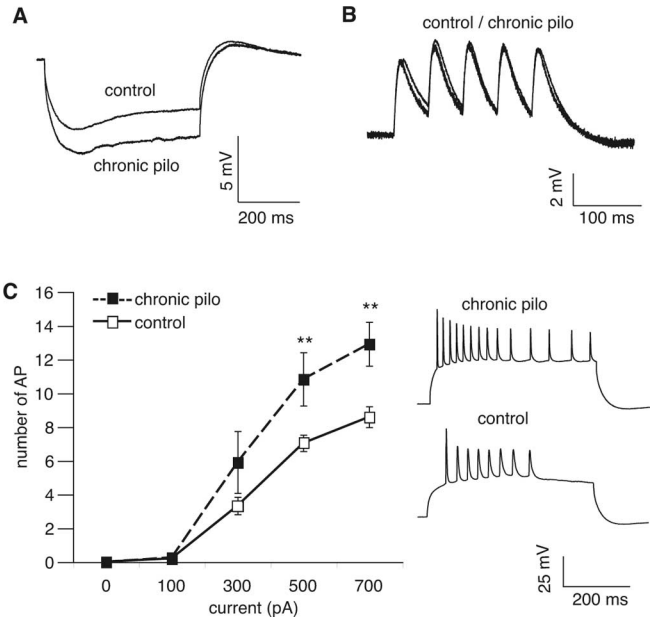

Figure 6. Increased IR and dendritic AP firing in the chronic period postpilocarpine. ***A***, Representative current-clamp recordings in response to 100 pA hyperpolarizing current injection demonstrated increased IR in pyramidal neuron dendrites from pilocarpine-treated animals. All measurements were performed with resting potential held at −65 mV, and dendritic recording distances in naive and pilocarpine-treated animals were 160 and 180 μm, respectively. ***B***, Representative traces show unchanged TS in dendritic current-clamp recordings at 160 and 170 μm in naive and pilocarpine-treated animals, respectively. All measurements were performed with resting potential held at −65 mV. ***C***, AP firing with depolarizing current injections (500 ms) showed increased excitability in pyramidal neuron dendrites from pilocarpine-treated animals in the chronic period compared with naive animals (**$p < 0.01$). Representative traces show enhanced dendritic AP firing with current injection of 700 pA in pyramidal neuron dendrites from epileptic animals compared with that from naive animals. The dendritic recording distances in naive and pilocarpine-treated animals were 180 and 170 μm, respectively.

Discussion

A number of studies have shown altered expression or biophysical properties of ion channels after SE in animal models during either the acute time period postinduction (Shah et al., 2004; Sanchez et al., 2005; Zhang et al., 2006), during chronic periods following the establishment of spontaneous seizures (Su et al., 2002; Ellerkmann et al., 2003; Bernard et al., 2004), or during both acute and chronic periods (Brooks-Kayal et al., 1998; Chen et al., 2001; Brewster et al., 2002; Peng et al., 2004). These studies provided important evidence that ion channel dysfunction occurs in animal models of acquired epilepsy. However, it has been unclear how the development of acquired alterations in ion channel activity correlated with the onset of spontaneous seizure activity. This is because, in some studies, seizures were not monitored, or because in other studies, only visual observation of convulsive activity was used, raising the possibility of undetected subtle seizures. Observing the correlation of acquired ion channel dysfunction and the onset of spontaneous seizures in animal models of epilepsy is necessary to understand whether channelopathy is a cause or effect of seizures. To answer this question, we investigated the properties of HCN channels in hippocampal pyramidal neurons using electrophysiological and biochemical

techniques in conjunction with VEEG monitoring. Our results showed that dendritic HCN channels were substantially downregulated at both acute and chronic time points after pilocarpine-induced SE. There were two separate mechanisms of HCN channel downregulation: a loss of HCN channel expression in the apical dendrites that was similar at acute and chronic time points, and altered HCN channel gating properties manifested by a hyperpolarizing shift in dendritic I_h voltage-dependent activation that progressively increased from acute to chronic periods. In parallel with HCN channel downregulation, VEEG recordings demonstrated that during the acute period, a significant fraction of pilocarpine-treated animals were already experiencing spontaneous seizures. Surprisingly, blockade of these seizures with PB revealed that the change in HCN channel-gating properties was dependent on this spontaneous seizure activity, whereas the loss of HCN channel expression was not. Thus, HCN channel dysfunction after SE represents multiple mechanisms, with potentially differing roles in seizures and epileptogenesis.

This study is the first to examine HCN channel function in hippocampal pyramidal dendrites after SE, and one of the first to correlate any acquired ion channel change with the development of epilepsy using VEEG techniques. The use of cell-attached voltage-clamp recordings to measure I_h allowed us to determine which of the different biophysical parameters of HCN channel function were altered during epileptogenesis. The loss of dendritic HCN channel expression was manifested by an ~50% decrease in I_h density. The similar loss in HCN protein expression suggests that the decreased I_h density reflects a decreased total number of HCN channels rather than alteration of single HCN channel conductance or a reduction only of HCN channels expressed at the membrane surface. Although we did not explore the mechanisms underlying this loss of channel expression, a previous study has shown a downregulation of HCN1 transcription at 1 week post-SE (Brewster et al., 2002), which suggests a possible transcriptional basis, whereas other translational and posttranslational mechanisms are possible. Altered HCN channel gating was shown by a hyperpolarization of I_h voltage-dependent activation and slowing of activation time constants. These changes reduce the amount of I_h active at neuronal resting potential and slow its recruitment by hyperpolarizing voltage transients. Of note, altered HCN channel function was detected only in dendritic regions, where HCN channels are predominantly localized, with no changes in current density or gating seen at the cell soma. This is in distinction to a previous study using the hyperthermic seizure model (Chen et al., 2001); however, whereas a subsequent study has shown that some animals undergoing hyperthermic seizures develop epilepsy at later time points (Dube et al., 2006), in the previous study, it was unknown whether the animals had become epileptic or not.

The HCN channel downregulation seen here would be predicted to cause pyramidal neuron hyperexcitability, as shown by a number of previous studies (Magee, 1999; Poolos et al., 2002, 2006). In this study, current-clamp measures of excitability were primarily consistent with previous results, with increased input resistance and action potential firing. However, temporal summation, a parameter influenced by I_h, was unaffected, suggesting that other voltage-gated conductances may be altered in chronic epilepsy that oppose the effects of decreased I_h, for example, the upregulation of voltage-gated potassium currents after SE (Park et al., 2006). It is likely that the hyperexcitability mediated by HCN channel downregulation contributes to the generation of spontaneous seizures, because previous studies have shown that knock-out of the HCN2 channel causes generalized epilepsy (Ludwig et al., 2003), and an antiepileptic drug effective for both focal and generalized epilepsy syndromes acts to upregulate I_h, among other actions (Poolos et al., 2002). Thus, at a minimum, HCN channel downregulation after pilocarpine-induced SE likely contributes to the epileptic phenotype by inducing intrinsic hyperexcitability in pyramidal neurons of hippocampus and neocortex.

An important question is whether the two mechanisms of HCN channel downregulation observed here contribute to epileptogenesis, or the development of the epileptic state after an acute insult such as SE. Our VEEG recordings show that this is a difficult question to answer definitively. Animal models of epilepsy using SE as the provoking insult ["postseizure" models (McNamara et al., 2006)] have found a "latent period" between SE and the appearance of spontaneous seizures; because ion channel changes occurring in the latent period are assumed independent of spontaneous seizures, it has been concluded that such changes (if they promote hyperexcitability) may be contributing to the process of epileptogenesis. Initial experience with the pilocarpine model of SE-induced epilepsy had shown the latent period to average ~15 d (Leite et al., 1990); however, there is wide variability in that measure, dependent in part on whether only visual observation is used to detect seizures with overt behavioral manifestations (i.e., Racine class 3–5 seizures). Our analysis of prolonged VEEG recordings showed that pilocarpine-treated animals began having seizures as early as day 3, and at least 40% were epileptic by day 6. Recent work by other investigators using VEEG techniques has shown a similar median latency period of ~6 d (Goffin et al., 2007), implying that at least half of the animals became epileptic within 6 d. Thus, in the pilocarpine model at least, the latent period may only last several days post-SE. The unexpected brevity of the latent period substantially narrows the window of time where post-SE ion channel changes can play an epileptogenic role. We observed HCN channel loss at 1 week postpilocarpine that was independent of spontaneous seizures. These results, plus previous findings of acute HCN channel loss post-SE (Shah et al., 2004) suggest that HCN downregulation may contribute to epileptogenesis. Even so, ion channel changes seen just 1 or 2 d post-SE may be merely a consequence of SE itself, and may not be epileptogenic per se. Proof that this acute HCN channel loss contributes in a causative manner to epileptogenesis will depend on a demonstration that reversal of HCN channel downregulation alters the course of epileptogenesis, a line of experimentation that was beyond the scope of this study. Nonetheless, we feel these results demonstrate the importance of VEEG techniques in verifying the course of epileptogenesis in conjunction with analysis of altered ion channel function, so to exclude ion channel dysfunction that is caused by, rather than a cause of, spontaneous seizures.

In contrast to HCN channel loss, the altered HCN channel gating observed in the first week postpilocarpine was shown to result from the onset of spontaneous seizures. This mechanism of HCN channel downregulation is therefore unlikely to be causative of epileptogenesis. However, it may contribute to maintaining or exacerbating the epileptic state, because its promotion of neuronal hyperexcitability could function in a positive-feedback cycle (McNamara et al., 2006). Recent insights into the modulation of I_h voltage-dependent activation by phosphorylation suggest some possible mechanisms for this seizure-dependent downregulation of HCN channel function (Poolos et al., 2006; Zolles et al., 2006; Fogle et al., 2007), similar to the phosphorylation-dependent upregulation of Kv2.1 gating after seizures (Park et al., 2006). It is interesting to note other work showing activity-

dependent upregulation of I_h during induction of synaptic plasticity (van Welie et al., 2004; Fan et al., 2005). This opposite change in HCN channel function induced by relatively brief periods of synaptic stimulation likely uses a different mechanism than the downregulation caused by the more intense synaptic stimulation associated with seizures.

This study adds to the growing literature linking ion channel dysfunction and epilepsy. A causative link between channelopathy and inherited epilepsy has been conclusively demonstrated for a number of human epilepsy syndromes. Our understanding of channelopathy in acquired epilepsy is also expanding, with identification of new candidates such as the HCN channel. Although the causative role of any of these alterations in ion channel function has yet to be proven, dissecting the signaling pathways underlying acquired channelopathy may provide novel insights into the molecular mechanisms of development of epileptic state and suggest pharmacologic targets for the prevention and treatment of epilepsy.

References

Arida RM, Scorza FA, Peres CA, Cavalheiro EA (1999) The course of untreated seizures in the pilocarpine model of epilepsy. Epilepsy Res 34:99–107.

Bernard C, Anderson A, Becker A, Poolos NP, Beck H, Johnston D (2004) Acquired dendritic channelopathy in temporal lobe epilepsy. Science 305:532–535.

Brewster A, Bender RA, Chen YC, Dube C, Eghbal-Ahmadi M, Baram TZ (2002) Developmental febrile seizures modulate hippocampal gene expression of hyperpolarization-activated channels in an isoform- and cell-specific manner. J Neurosci 22:4591–4599.

Brooks-Kayal AR, Shumate MD, Jin H, Rikhter TY, Coulter DA (1998) Selective changes in single cell GABA(A) receptor subunit expression and function in temporal lobe epilepsy. Nat Med 4:1166–1172.

Chen K, Aradi I, Thon N, Eghbal-Ahmadi M, Baram TZ, Soltesz I (2001) Persistently modified h-channels after complex febrile seizures convert the seizure-induced enhancement of inhibition to hyperexcitability. Nat Med 7:331–337.

D'Ambrosio R, Fairbanks JP, Fender JS, Born DE, Doyle DL, Miller JW (2004) Post-traumatic epilepsy following fluid percussion injury in the rat. Brain 127:304–314.

Day M, Carr DB, Ulrich S, Ilijic E, Tkatch T, Surmeier DJ (2005) Dendritic excitability of mouse frontal cortex pyramidal neurons is shaped by the interaction among HCN, Kir2, and k(leak) channels. J Neurosci 25:8776–8787.

Dube C, Richichi C, Bender RA, Chung G, Litt B, Baram TZ (2006) Temporal lobe epilepsy after experimental prolonged febrile seizures: prospective analysis. Brain 129:911–922.

Ellerkmann RK, Remy S, Chen J, Sochivko D, Elger CE, Urban BW, Becker A, Beck H (2003) Molecular and functional changes in voltage-dependent Na^+ channels following pilocarpine-induced status epilepticus in rat dentate granule cells. Neuroscience 119:323–333.

Fan Y, Fricker D, Brager DH, Chen X, Lu HC, Chitwood RA, Johnston D (2005) Activity-dependent decrease of excitability in rat hippocampal neurons through increases in I_h. Nat Neurosci 8:1542–1551.

Fogle KJ, Lyashchenko AK, Turbendian HK, Tibbs GR (2007) HCN pacemaker channel activation is controlled by acidic lipids downstream of diacylglycerol kinase and phospholipase A2. J Neurosci 27:2802–2814.

Goffin K, Nissinen J, Van Laere K, Pitkanen A (2007) Cyclicity of spontaneous recurrent seizures in pilocarpine model of temporal lobe epilepsy in rat. Exp Neurol 205:501–505.

Hsieh PF, Watanabe Y (2000) Time course of c-FOS expression in status epilepticus induced by amygdaloid stimulation. NeuroReport 11:571–574.

Leite JP, Bortolotto ZA, Cavalheiro EA (1990) Spontaneous recurrent seizures in rats–an experimental-model of partial epilepsy. Neurosci Biobehav Rev 14:511–517.

Lubin FD, Ren Y, Xu X, Anderson AE (2007) Nuclear factor-κB regulates seizure threshold and gene transcription following convulsant stimulation. J Neurochem 103:1381–1395.

Ludwig A, Budde T, Stieber J, Moosmang S, Wahl C, Holthoff K, Langebartels A, Wotjak C, Munsch T, Zong XG, Feil S, Feil R, Lancel M, Chien KR, Konnerth A, Pape HC, Biel M, Hofmann F (2003) Absence epilepsy and sinus dysrhythmia in mice lacking the pacemaker channel HCN2. EMBO J 22:216–224.

Lupica CR, Bell JA, Hoffman AF, Watson PL (2001) Contribution of the hyperpolarization-activated current (I_h) to membrane potential and GABA release in hippocampal interneurons. J Neurophysiol 86:261–268.

MacDonald RL, McLean MJ (1986) Anticonvulsant drugs: mechanisms of action. Adv Neurol 44:713–736.

Magee JC (1998) Dendritic hyperpolarization-activated currents modify the integrative properties of hippocampal CA1 pyramidal neurons. J Neurosci 18:7613–7624.

Magee JC (1999) Dendritic l_h normalizes temporal summation in hippocampal CA1 neurons. Nat Neurosci 2:508–514.

McNamara JO, Huang YZ, Leonard AS (2006) Molecular signaling mechanisms underlying epileptogenesis. Sci STKE 2006:re12.

Park KS, Mohapatra DP, Misonou H, Trimmer JS (2006) Graded regulation of the Kv2.1 potassium channel by variable phosphorylation. Science 313:976–979.

Peng ZC, Huang CS, Stell BM, Mody I, Houser CR (2004) Altered expression of the delta subunit of the $GABA_A$ receptor in a mouse model of temporal lobe epilepsy. J Neurosci 24:8629–8639.

Poolos NP, Johnston D (1999) Calcium-activated potassium conductances contribute to action potential repolarization at the soma but not the dendrites of hippocampal CA1 pyramidal neurons. J Neurosci 19:5205–5212.

Poolos NP, Migliore M, Johnston D (2002) Pharmacological upregulation of h-channels reduces the excitability of pyramidal neuron dendrites. Nat Neurosci 5:767–774.

Poolos NP, Bullis JB, Roth MK (2006) Modulation of h-channels in hippocampal pyramidal neurons by p38 mitogen-activated protein kinase. J Neurosci 26:7995–8003.

Racine RJ (1972) Modification of seizure activity by electrical stimulation. II. Motor seizure. Electroencephalogr Clin Neurophysiol 32:281–294.

Sakmann B, Neher E (1995) Geometric parameters of pipettes and membrane patches. In: Single-channel recording (Sakmann B, Neher E, eds), pp 637–650. New York: Plenum.

Sanchez RM, Dai WM, Levada RE, Lippman JJ, Jensen FE (2005) AMPA/kainate receptor-mediated downregulation of GABAergic synaptic transmission by calcineurin after seizures in the developing rat brain. J Neurosci 25:3442–3451.

Santoro B, Tibbs GR (1999) The HCN gene family: molecular basis of the hyperpolarization-activated pacemaker channels. Ann NY Acad Sci 868:741–764.

Shah MM, Anderson AE, Leung V, Lin XD, Johnston D (2004) Seizure-induced plasticity of h channels in entorhinal cortical layer III pyramidal neurons. Neuron 44:495–508.

Steinlein OK (2004) Genetic mechanisms that underlie epilepsy. Nat Rev Neurosci 5:400–408.

Su H, Sochivko D, Becker A, Chen J, Jiang YW, Yaari Y, Beck H (2002) Upregulation of a T-type Ca^{2+} channel causes a long-lasting modification of neuronal firing mode after status epilepticus. J Neurosci 22:3645–3655.

van Welie I, van Hooft JA, Wadman WJ (2004) Homeostatic scaling of neuronal excitability by synaptic modulation of somatic hyperpolarization-activated Ih channels. Proc Natl Acad Sci USA 101:5123–5128.

Varga AW, Anderson AE, Adams JP, Vogel H, Sweatt JD (2000) Input-specific immunolocalization of differentially phosphorylated Kv4.2 in the mouse brain. Learn Mem 7:321–332.

Velumian AA, Zhang L, Pennefather P, Carlen PL (1997) Reversible inhibition of I_k, I_{AHP}, I_h and I_{Ca} currents by internally applied gluconate in rat hippocampal pyramidal neurones. Pflügers Arch 433:343–350.

Zhang K, Peng BW, Sanchez RM (2006) Decreased I-H in hippocampal area CA1 pyramidal neurons after perinatal seizure-inducing hypoxia. Epilepsia 47:1023–1028.

Zolles G, Klocker N, Wenzel D, Weisser-Thomas J, Fleischmann BK, Roeper J, Fakler B (2006) Pacemaking by HCN channels requires interaction with phosphoinositides. Neuron 52:1027–1036.